Determination of Residual Stress of PACVD Nanostructure TiN Coatings by GIXRD Method

M. Raoufi[1,*], A. Zolanvari[2], M. Zarezadeh Mehrizi[1]

[1] Department of Materials Science and Engineering, Faculty of Engineering, Arak University, Arak 38156-8-8349, Iran.
[2] Department of Physics, Faculty of Science, Arak University, Arak, Iran.

ARTICLE INFO

Article history:

Received 4 July 2017
Accepted 14 October 2018
Available online 5 November 2018

Keywords:

TiN
Plasma assisted chemical vapor deposition
Residual stress
GIXRD

ABSTRACT

In this study, thin layers of titanium nitride (TiN) were deposited on H13 steel substrates at different duty cycles and temperature of 520˚C using plasma assisted chemical vapor deposition (PACVD). Uniaxial residual stress was calculated by X-ray diffraction (XRD) and Sin2 Ψ method. Then the residual stress of the samples were measured by Grazing Incidence X-ray Diffraction (GIXRD) method and lattice parameter diagrams versus f(Ψ). Depth of penetration and texture coefficient in the samples were also evaluated. The surface morphology was examined using field-emission gun scanning electron microscope (FESEM) and the relationship of the stress and micro hardness test was also expressed. The results showed that by reducing duty cycles, residual stress decreases as well as with more changes of the lattice parameter, more changes of residual stress will be seen. Also, the microstructure result was in good agreement with theory and clearly displayed spherical morphology and uniform distribution of the created phases.

1-Introduction

Nowadays, TiN coatings have been extensively used in industrial applications like protection of cutting tools and forming and decorative applications due to their unique characteristics like high hardness, high corrosion and wear resistance as well as golden appearance [1]. One of the mechanical properties which is effective on the control of these factors is residual stress. The fracture of the coatings through the formation of holes and cracks and loss of adhesion is related to the type and magnitude of residual stresses [2]. TiN layers have been produced and evaluated by different methods which include magnetron sputtering [3,4], evaporation [5], ion plating [6], reactive ion beam [2], plasma immersed ion implantation [7]. Novotna et al. [8] couldn't succeed to calculate residual stresses of the produced TiN layers by sputtering method due to low intensities of TiN peaks which seems deposition has not been implemented well. Gomez et al. [3] obtained minimum residual stress at incident angle of 1.5˚ (-3 Gpa) by GIXRD method. In this study by applying low bios voltage such value was observed. Hernandes et al. [5] were deposited TiN layers on the steel by evaporation method (electric arc) and achieved compressive stress (-3 Gpa) by increasing bios voltage. King et al. [2] confirmed this result using reactive ion method
by increasing the temperature to 800˚C and cooling to room temperature. Matsue et al. [6] were reported residual stress (-3.5 Gpa) by heating the sample and applying bios voltage. According to this study, this residual stress

* Corresponding author:
E-mail address: m-raoufi@araku.ac.ir

arises from ion bombardment and is intrinsic. This reduction of stress during firing is as a result of strain relief related to the inherent stress. Liu et al. [7] were deposited TiN layers using plasma immersed ion implantation and reported residual stress of -1.163 GPa by GIXRD analysis and increasing the thickness of the layer. PVD processes which have been mentioned above possess directional nature and don't provide coating of the samples having complex geometric shapes. The processing temperature of CVD is about 1000 ˚C which is higher than tempering temperature of the steel and causes reduction of the strength of substrate after processing. These two limitations justify use of plasma for chemical vapor deposition. Application of plasma in CVD process decreases the temperature of the process by the production of ions and free radicals. Thus, PACVD process has provided development of hard layers against corrosion and wear including deposition of TiN layers on steel samples with complex geometrics at temperatures lower than their tempering temperature [9]. The residual stress in hard coatings affects the wear resistance [10].

The residual stresses in TiN layers which have been developed by PACVD method have not been evaluated yet. This study is aimed to evaluate residual stresses in these layers.

2-Materials and Methods

Three disc samples with diameter of 5 cm and thickness of 8 cm were provided from H13 steel bars. Then, the samples were machined by magnetic grinding and polished by sand papers. In order to obtain good surface finishing, samples were polished with alumina powders of 0.5 μm and then washed with distilled water and alcohol and dried rapidly by hot air blowing. In order to obtain suitable structural strength, the samples were subjected to quench and tempering processes before plasma processing. Tempering process was performed on the samples for 1 h at 550˚C to remove created stresses.

After heat treating the samples, plasma assisted chemical vapor deposition was performed on the samples. This process was done in PACVD instrument. The samples were coated by TiN at 520˚C and three different duty cycles of 33%, 40% and 50%. The stress in the samples was calculated by XRD instrument (PANalytical X'Pert PRO XRD (Philips Analytical BV, Almelo, The Netherlands) using Cu Kα radiation with λ = 0.15406 nm) using Sin2ψ method and X' Pert Stress software.

In order to analyze the coatings by XRD at low angles (GIXRD), small samples were cut in to 1cm × 1 cm dimensions by EDM machining and then were thinned by electrical discharge process. In order to examine the TiN coating, GIXRD method is used due to very thin thickness of the coating and that only the coating would be examined. In order to better characterize the available phases and use of X-ray elastic constants to calculate residual stress, X-ray diffractometer of Panalytical Co. (X'Pert Pro MPD model) was used. The diffractions of all samples at incidence angle of 2θ between 5-85˚ have been done continuously. The positions of the samples were held on constant angle of (W) and the detector was recorded different diffraction peaks related to reflection (hkl) planes. The incidence angles of X-ray with the surface of the sample were selected at 1, 3 and 5˚. This test was performed by Cu K_α radiation with wavelength of 1.54 A˚, voltage of 40 kw, current of 40 mA and step of 0.039 angle/sec. The surface morphology of the samples with 33% duty cycle was examined by FE-SEM (MIRA3 TESCAN). In order to measure the hardness of the sample's coatings, Shimadzo micro-hardness instrument and load of 50 gr was used to obtain just the hardness of the coatings. Every sample was evaluated by hardness test 5 times at least and the average value was reported as the hardness of the sample. The hardness tests were done at enough distances with each other to prevent the test error.

3-Results and Discussion

In order to evaluate TiN coatings, GIXRD method was used. This method was selected due to its ability to characterize the available phases at surficial layers. Samples which have been coated by TiN at 520˚C and duty cycles of 33%, 40% and 50% were evaluated by this method. As can be seen in Fig. 1 and 2, TiN peaks are observed at 36.8, 42.8, 62, 74.4 and 78.1 angles and are consistent with TiN powder peaks according to standard reference (JCPDS 38-1420). These peak positions correspond to crystallographic planes of (111), (200), (220),

(311) and (222), respectively. The incident angle was selected between 1 to 5˚, so the depth of X-ray penetration was different for different samples. The depth of X-ray penetration was calculated based on the Eq. (1).

$$Xe = \frac{\sin w.\sin(2\theta - w)}{\mu[\sin w + \sin(2\theta - w)} \quad (1)$$

In which Xe is the depth of penetration, w and is incident angle, 2θ is the brag angle and μ is linear absorption coefficient which its value for the ideal structure of TiN without any defects is 876 cm^{-1}. The penetration depth for incident angles of 1, 3 and 5˚ was calculated and represented in Table (1). As can be seen in Table (1), by the increase of incident angle to 5˚ at constant 2θ as well as increase of 2θ angles at constant w, increase of penetration depth is obviously seen. As can be seen in Table (1), by the increase of w, 2θ is getting closer to its actual value according to standard reference (JCPDS 39-1420) because more planes were detected. The degree of preferred direction of TiN coating growth for different planes using texture coefficient (Tc) is defined as the following [11]:

$$T_c = \frac{I_m(hkl)/I_0(hkl)}{\frac{1}{n}\sum_1^n I_m(hkl)/I_0(hkl)} \quad (2)$$

In which I_m(hkl) is the reflection intensity of (hkl) crystalline planes from the coating, I_0(hkl) is the reflection intensity for the reference sample and n is the sum of the number of reflections.

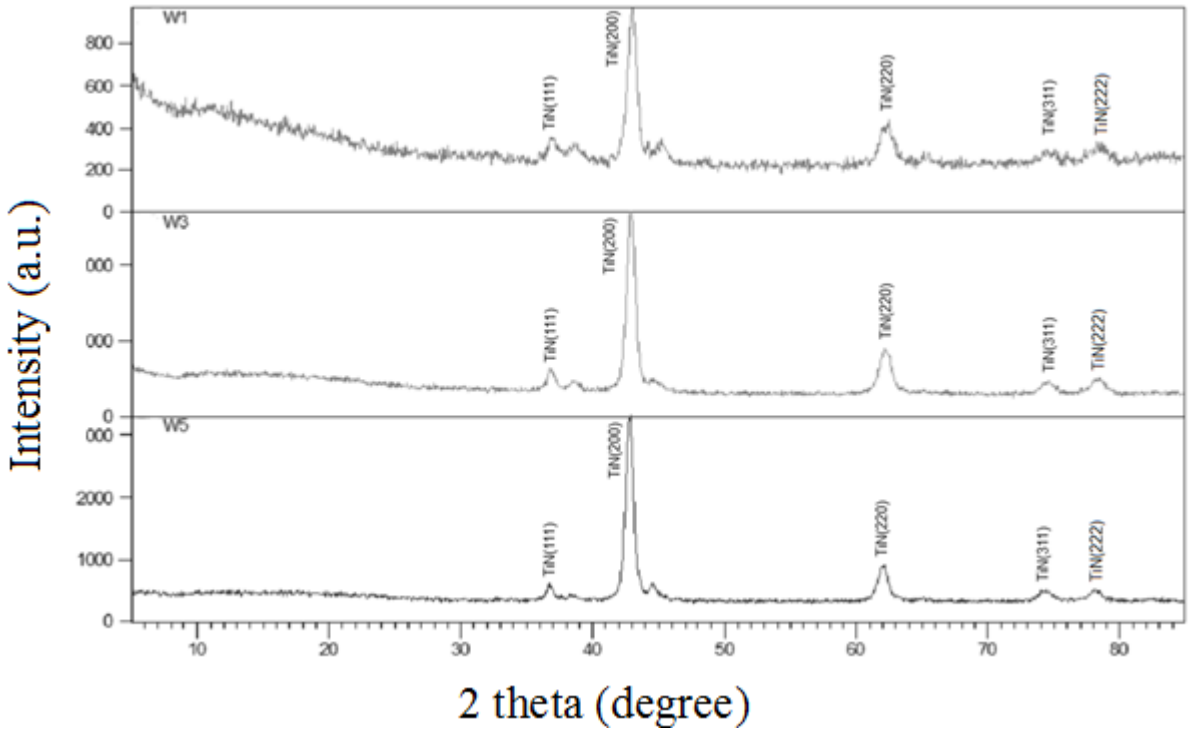

Fig. 1. GIXRD diagrams of TiN coating at duty cycle of 33%.

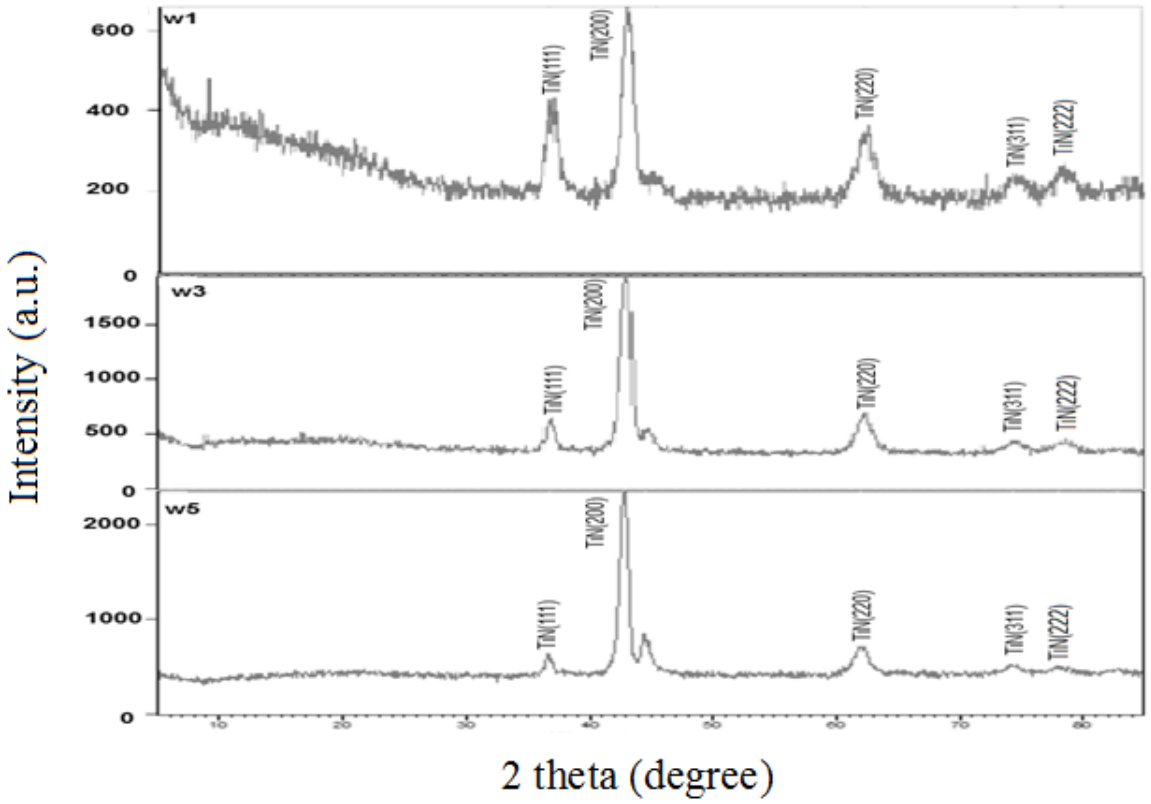

Fig. 2. GIXRD diagrams of TiN coating at duty cycle of 50%.

Table1. Change of penetration depth versus 2θ and w at duty cycle of 33%.

2θ(°) ,w=1	Penetration depth (μm)	2θ(°) ,w=3	Penetration depth (μm)	2θ(°) ,w=5	Penetration depth (μm)
36.846	0.1893	36.83	0.5459	36.73	0.8544
42.988	0.1936	42.882	0.5518	42.77	0.8545
62.250	0.1941	62.165	0.5633	61.967	0.9012
74.620	0.1941	74.46	0.565	74.27	0.9094
78.453	0.1942	78.27	0.5661	78.09	0.822

The values of texture coefficient which have been represented in Table (2), showed that the preferred direction of growth for TiN coating was the normal of (200) plane that its value for duty cycle of 33% was more than that of duty cycle of 50%. In addition, the diffraction intensity of (200) planes at GIXRD diagrams supports it. The value of T_c(hkl) =1 indicated the crystalline layers with random orientations whereas higher values suggest abundance of oriented grains at certain direction of (hkl). Actually, reduction of duty cycles caused to increase of texture coefficient at (200) planes and this behavior suggested improved preferred orientation of (200) planes as a result of the reduction of duty cycle. The preferred directions for TiN coatings which have been deposited from evaporated phase changed with the growing conditions [11]. For example, the wear resistance of cutting tools depends on the direction of TiN coating growth as [111] direction is known as the direction which has the highest wear resistance in such coatings [12]. Pelleg et al. suggested that the driving force which causes growth at preferred directions for thin layers of TiN arises from minimum energy that is composed of surficial and strain energy [13].

Table 2. Values of texture coefficient of the matrix for crystalline planes at different duty cycles.

T_c (222)	T_c (311)	T_c (220)	T_c (200)	T_c (111)	Duty cycle (%)
1.0481	0.7051	0.9194	2.12	0.2067	33
0.6477	0.7554	0.7815	2.1498	0.6651	40
0.9723	0.6419	0.9395	1.8999	0.5459	50

They predicted that when the surface energy is dominant, the preferred direction of growth of TiN coating is (200) plane having least surficial energy and when the strain energy is dominant, the preferred direction of growth is (111) plane with least strain energy. Recently, other authors also confirmed this model of surface and strain energy [14-15]. Diffraction patterns showed that the degree of preferred growth was (200) plane and this implies that during the growth of the layer, the state of surficial energy was dominant. However, for TiN coatings which have been deposited using magnetic sputtering, the preferred direction of the layer is (111) plane [16]. Particles were created with greater momentum in magnetic sputtering in compared to PACVD method [17].

The intrinsic stresses within the layers which are created by bombardment of particles depend on their momentum [18]. Therefore, the layers which are created by magnetic sputtering have greater intrinsic stress and strain energy than thin layers which are deposited by PACVD method. Therefore, it is expected that atoms arrange at planes with lower strain energy namely (111) planes so that finally, the energy of the created layer would have the least amount [18]. According to the aforementioned discussion, the atomic arrangement of TiN layer by PACVD method at (200) planes is not unexpected and is completely consistent with theoretical discussion.

GIXRD method also was used to measure the diameter of crystallites of the layers. The geometry of the GIXRD analysis is represented in Fig. 3. The diameters of crystallites were calculated by Willamson-Hall equation (Eq. (3)) which their values are expressed in Table (3) [15].

$$\beta \cos\theta = \frac{0.91\lambda}{d} + 2A\varepsilon \sin\theta \quad (3)$$

Where β is the full width of the peak at half maximum (FWHM) and λ is the wavelength of the used X-ray.

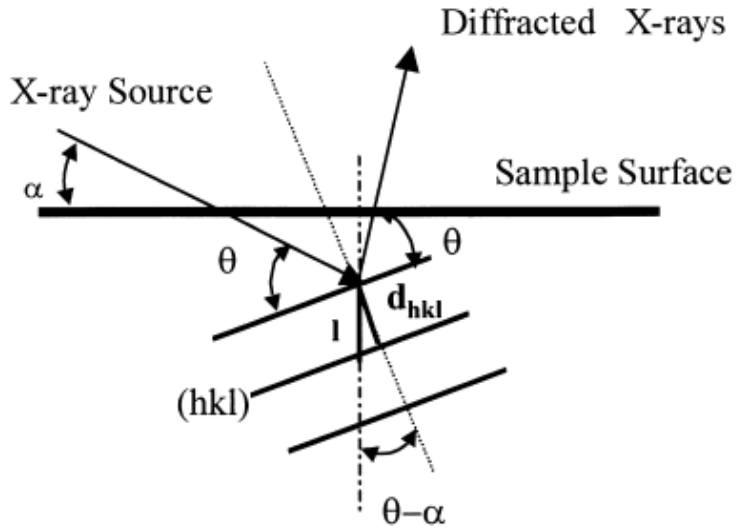

Fig. 3. Orientation of diffraction planes versus sample surface.

For a certain peak position of 2θ which corresponds to diffraction peak of (hkl) plane, ψ is the angle between a line perpendicular to the sample plane and the line perpendicular to diffraction plane of (hkl) which is defined as:

$$\psi = \theta - w \tag{4}$$

In order to calculate the residual stress at the surface, it is supposed that the available stresses at the layer possess biaxial state. In this regard, the following equation is valid for determination of lattice parameter (a) and residual stress (σ) [12-13]:

$$a = a_0(\sigma f(\psi) + 1)$$

$$f(\psi) = \frac{1}{2} S_{2hkl} \sin 2\psi + 2S_{1hkl} \tag{5}$$

In these equations, ψ angle is related to the diffraction angle of (hkl) planes and a_0 is the lattice parameter with no stress. Elastic constants of X-ray ($2S_1$, ½ S_2) for different (hkl) planes of TiN layer have been represented in Table 3. Thus, with the help of obtained values for lattice parameter, diagram of (a) versus f(ψ) can be plotted for different (hkl) planes. Assuming a linear relationship between the lattice parameter (a) and f (ψ) in equation (5) must be kept, σ values can be calculated by y-intercept of lattice constant a_0 as well as slope of the diagram. Fig. 4 showed the plotted diagrams for different conditions of deposition to calculate a_0 and σ. According to the following equation that expresses the relationship of lattice parameter and inter-planar distance, lattice parameter (a) can be obtained [15]:

$$d = \frac{a}{\sqrt{h^2 + k^2 + l^2}} \tag{6}$$

According to the standard (JCPDS 38-1420) and in powder state, the size of the lattice parameter is 4.24 A˚. The values of lattice parameter which have been obtained from equation (6) and with respect to the diagram differ from standard state. One of the reasons of the difference in lattice parameter can be caused by impurities. For example, if these impurities would be carbon or chlorine atoms could increase the lattice parameter whereas if hydrogen or oxygen atoms would be as impurities, decrease of lattice parameter occurs. In addition, due to the formation of vacancies, lattice parameters for non-stoichiometric layers decreases.

In this study, the calculated value of lattice parameter for the formed thin layer in most cases was smaller than the values which have been reported for this structure with perfect lattice and without defects. This can be due to nitrogen vacancies. Because of the effect of sputtering process, nitrogen atoms which are lighter than titanium atoms were detached easier from the surface and create nitrogen vacancies [11].

The values of residual stress in the samples before cutting were obtained using Sin2ψ method (Table 3). It is observed that by the increase of duty cycle, the value of residual compressive stress increased but hardness unlikely decreased. Thus, increase of hardness through residual stress was not justified. Raoufi et al. [19], have reported that with the increase of duty cycle, the roughness of the surface increase and hardness decreases. By the increase of roughness, unevenness of the sample surface increases and conjunctions of the atoms will be less and as a result hardness decreases. The residual stress was also calculated using GIXRD method after cutting. As can be observed from Table (3), reduction of duty cycle from 50% to 40% leads to the increase of residual compressive stress.

It is worth to note that with increasing the changes of the lattice parameter after cutting at w=1 in compared to before cutting, further increase of residual stress is obvious that is not unexpected. While with the increase of residual stress (compressive or tensile) in the material, because the atoms are pressed to each other, external object can force hardly into the material and suggests more hardness. In other words, by the increase of residual stress, achieving high hardness in not unexpected and as can be seen in Table (3), increase of hardness was consistent with the increase of compressive stress after cutting.

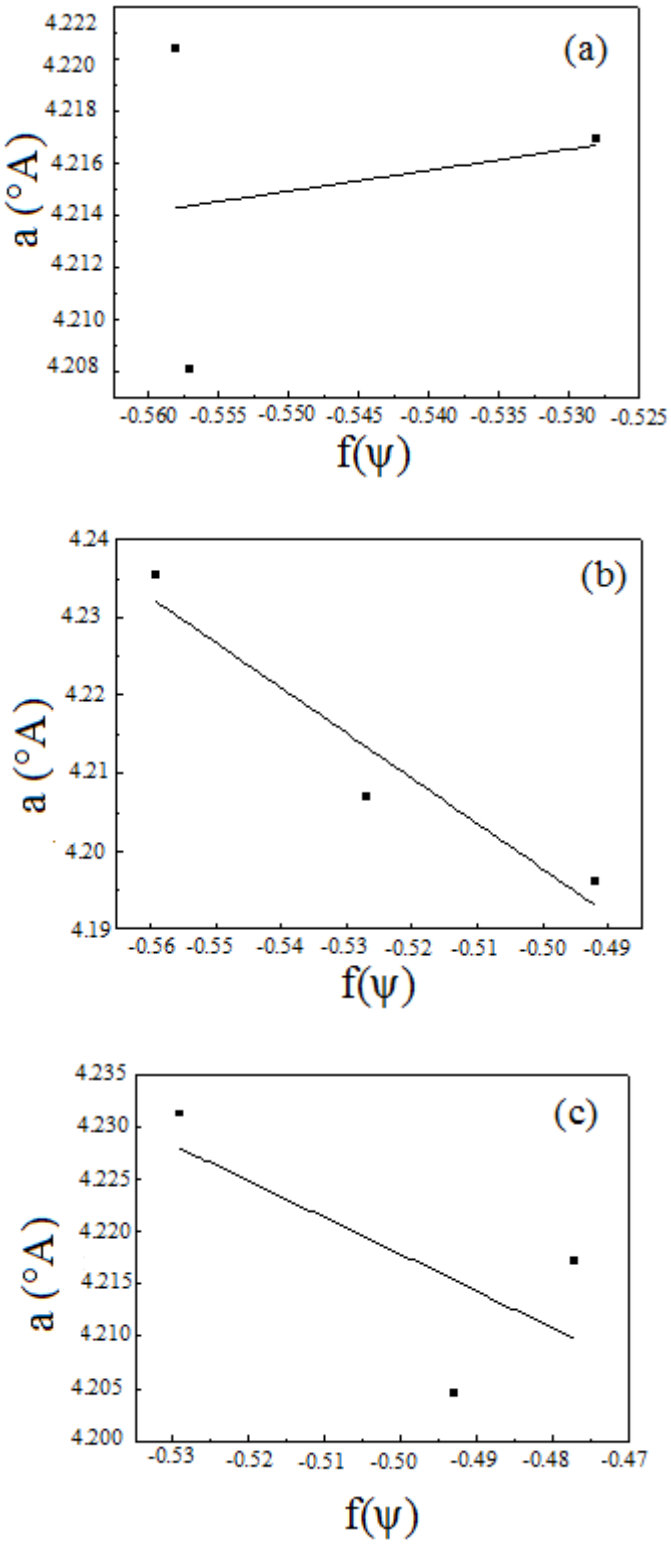

Fig. 4. change of lattice parameter versus f(ψ) at different duty cycles of deposition including a) 33% b) 40% and c) 50%.

Table 3. Comparison of residual stress of the layers before and after cutting by lattice parameter changes.

Calculate average grain size (nm)	hardness ($HV_{0.050}$)	Average crystallite size (200) (nm)	a_0 (A°)	Δa(A°)	a(A°), w=1	Stress after cutting (GPa)	a(A°)	Stress before cutting (GPa)	Duty cycle (%)
15	1798	15	4.2591	0.01	4.20	18	4.21	-1.4907	33
29	1732	28	3.9067	0.04	4.19	-148	4.23	1.282	40
30	1680	27	4.0428	0.03	4.20	-86.5	4.23	-6.1714	50

One of the mechanisms of increasing hardness, is the reduction of grain size (or increasing the amount of grain boundaries). According to Hall-Petch equation (equation (5)), hardness value varies inversely with the grain size. This means that reduction of grain size leads to the increase of material hardness.

$$H\alpha \frac{1}{\sqrt{D}} \quad (7)$$

In this equation, H is the final hardness of the material and D is the grain size of the coating. Table (3) represents the average grain sizes which have been obtained by Debye-Sherrer equation. It is observed that with the increase of duty cycle, grain size increases which was consistent with the reduction of the hardness.

Fig. 5 shows FE-SEM image of the surface of the sample at different magnifications which has been coated with TiN at duty cycle of 33%. As can be seen in Fig. 5, surface of the sample was composed of fine spherical TiN particles which were located together. As is observed, the particles which were seen as grain at lower magnifications, they were themselves composed of very finer grains. Actually, large grains of TiN have been created by the accumulation of finer TiN grains. The boundary between these small grains was very small and they were hardly distinguishable. The actual grain size was obtained 39 nm which is comparable with the value of debye-sherrer equation.

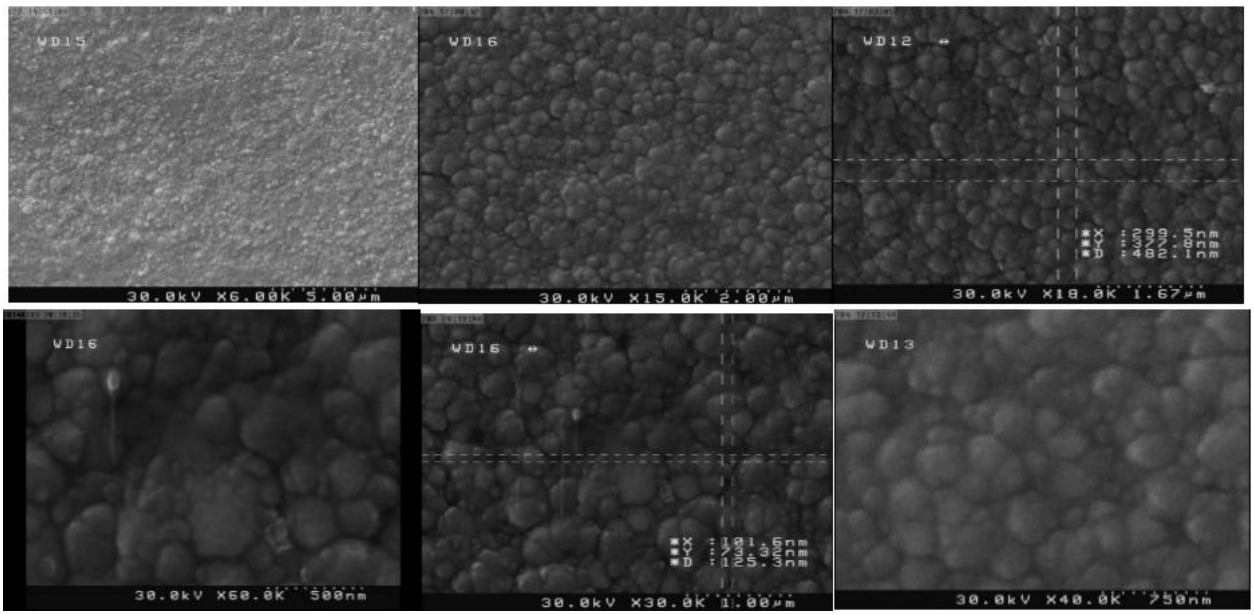

Fig.5. FESEM images of the sample at duty cycle of 33% with different magnification.

4. Conclusion

In this study, the residual stresses in TiN layers which have been developed by PACVD method have been evaluated. Based on the results, the following are obtained.

- By the reduction of duty cycle, texture coefficient of (200) increases which was not unexpected with respect to the reduction of residual stress because by the increase of texture coefficient, crystalline order of the coating increased and experienced lower pressure.
- By the reduction of duty cycle, residual stress decreased and hardness increased which was a tribological characteristic of a good compound.
- By the reduction of duty cycle, grain size decreased which was consistent with the increase of hardness.

References

[1] C. Mitterer, F. Holler, D. Reitberger, E. Badisch, M. Stoiber, C. Lugmair, R. Nobauer, Th. Muller, R. Kullmer, "Industrial applications of PACVD hard coatings", Surf. Coat. Technol., Vol. 163- 164, 2003, pp. 716- 722.

[2] H.W King, J.D Brown, T.A Caughlin, Temperature Dependence of Residual stress in TiN thin films on 316 stainless steel, JCPDS-International Centre for Diffraction Data, 1997.

[3] A.G. Gomez, A.A.C. Recco, and L.G. Martinez, Residual stress in TiN thin films studied by the grazing incidence X-ray diffraction method, LNLS Activity Report, 2007.

[4] R.O.E Vijen, J.H. Dautzenberg, "Mechanical measurement of the residual stress in thin PVD films", Thin Solid Films, Vol. 270, 1995, pp. 264-269.

[5] L.C Hernandes, L. Ponce, A. Fudora, E. Lopez and E.Perez, "Nanohardness and Residual stress in TiN coating", Materials, Vol. 4, 2011, pp. 929-940.

[6] T. Matsue, T. Hanabusa, K. Kusaka and O. sakata,"Relaxation of Residual stresses in Thin Films investigated using Synchrotron Radiation", JCPDS-International Centre for Diffraction Data, Vol. 29, pp. 233-239.

[7] H. Liu, Q. Xu, X. Zhang, Ch. Wang, B. Tang, Residual stress analysis of TiN film fabricated by plasma immersion ion implantation and deposition process, Elsevier, 2012.

[8] Z. Novotna, R. Kra lova , R. Nova k, J. Marek, "X-ray analysis of residual stresses in TiN coatings", Surf. Coat. Technol., Vol. 116-119, 1999, pp. 424–427.

[9] D. Heima, F. Hollerb, C. Mittererb, "Hard coatings produced by PACVD applied to aluminium die casting", Surf. Coat. Technol., Vol. 116-119, 1999, pp. 530–536.

[10] S. Zhang, H. Xie, X. Zeng, P. Hing, "Residual stress characterization of diamond-like carbon coatings by an X-ray diVraction method", Surf. Coat. Technol., Vol. 122, 1999, pp. 219–224.

[11] M.I. Jones, I.R. McColl, D.M. Grant, "Effect of substrate preparation and deposition conditions on the preferred orientation of TiN coatings deposited by RF reactive sputtering", Surf. Coat. Technol., Vol. 132, 2000, pp.143-151.

[12] D.R. McKenzie, Y.Yin, W.D. McFall, N.H. Hoang, "The orientation dependence of elastic strain energy in cubic crystals and its application to the preferred orientation in titanium nitride thin films", J.Phys. Cond Mater., Vol. 8, 1996, pp. 5883-90.

[13] J. Pelleg, L.Z. Zevin, S. Lungo, "Reactive Sputter Deposited Tin Films On Glass Substrates", Thin Solid Films, Vol. 197, 1991, pp. 117- 122.

[14] N.H. Hoang, D.R. McKenzie, D. R. McFall, Y. Yin, "Properties of Tin Thin films deposited at low temperature in a new plasma-based deposition systemJ. Appl. Phys., Vol. 80, 1996, pp. 6279-6285.

[15] B. Subramanian, K. Ashok, M. Jayachandran, "Effect of substrate temperature on the structural properties of magnetron sputtered titanium nitride thin films with brush platad nickel interlayer on mild steel", Appl. Surf. Sci., Vol. 255, 2008, pp. 2133-8.

[16] J. J. Cuomo, D. L. Pappas, J. Bruley, J. P. Doyle. and K. L. Saenger, "vapor deposition processes for amorphous carbon films with sp3 fractions approaching diamond", J. appl. phys., Vol. 70, 1991, pp. 1706-10.

[17] H. Windischmann, K.J. Gray, "Stress measurment of CVD diamond films", Diamond Relat. Mater., Vol. 4, 1995, pp. 837-842.

[18] U. C. Oh, J. H. Je, "effect of strain energy on the preferred orientation of TiN thin films", J. appl. Phys., Vol. 74, 1993, pp. 1692-6.
[19] M. Raoufi, Sh. Mirdamadi, F. Mahboubi, Sh. Ahangarani, M.S. Mahdipoor, H. Elmkhah, "Correlation between the surface characteristics and the duty cycle for the PACVD-derived TiN nanostructured films", Surf. Coat. Technol., Vol. 205, 2011, pp. 4980–4.